Fast steering mirror implementation for reduction of focal-spot wander in a long-distance free-space communication link

M.R. Suite[a], H.R. Burris[b], C.I. Moore[a], M.J. Vilcheck[a], R. Mahon[c], Carmen Jackson[b], M.F. Stell[b], M.A. Davis[d], W.S. Rabinovich[e], W.J. Scharpf[a], A.E. Reed[a], G.C. Gilbreath[f]

[a]U.S. Naval Research Laboratory, Code 8123, Advanced Systems Technology Branch, 4555 Overlook Ave SW, Washington, DC 20375;
[b]Research Support Instruments, Inc., 4325-B Forbes Blvd., Lanham, MD 20706;
[c]Jaycor/Titan, Inc., 1410 Spring Hill Rd., McLean, VA 22102;
[d]Honeywell T.S.I., 7515 Mission Drive, Lanham, MD 20706;
[e]U.S. Naval Research Laboratory, Code 5654, Photonics Technology Branch, 4555 Overlook Ave SW, Washington, DC 20375;
[f]U.S. Naval Research Laboratory, Code 7215, Radio/IR/Optical Sensors Branch, 4555 Overlook Ave SW, Washington, DC 20375;

ABSTRACT

One of the causes of power loss in a free-space optical communication link is beam motion or received spot wander. The power spectrum of the spot motion indicates that most of the frequency content is less than ~500 Hz. A fast steering mirror (FSM) controlled by a position-sensing detector (PSD) has the potential to correct for a significant portion of the focal spot position fluctuations and thus the power loss. A FSM controlled with a Germanium PSD was installed on the receiver at the NRL Chesapeake Bay free-space lasercomm test facility. Results are presented from the initial tests performed using this system to measure and correct for wander of an optical beam propagated across the bay (20 mile round-trip).

Keywords: free-space optical communication, laser communications, fast steering mirror

1. INTRODUCTION

Atmospheric turbulence has always limited the stability and quality of free-space laser communication links. Implementing a fast steering mirror (FSM) to actively compensate for the angle-of-arrival (AoA) fluctuations allows for a more robust link, even strong turbulence conditions. Implementation of an FSM is a known method to compensate for these conditions to improve signal reliability. In this work, we combined a PSD with an FSM to achieve this goal. The system was installed and tested at the NRL free space optical (FSO) communications test facility established at the Chesapeake Bay Detachment (CBD) of the Naval Research Laboratory (NRL)[1,2].

2. EXPERIMENTAL SETUP

One of the sites at the FSO facility has a laser transmitter and telescope-based receiver situated on a cliff about 30 meters above sea level. Located about 16.2 km away on a tower on Tilghman Island are target planes with retro-reflectors mounted in asymmetric distributions. It was this site that was used to test the FSM.

The laser transmitter available at the site is a 1550nm oscillator amplified to 1.6 watts in an erbium doped fiber amplifier developed by the Optical Sciences Division of NRL[3,4]. The beam is fiber-coupled to a 4" collimating lens on a remotely controlled Sagebrush gimbal mount. The receiver consists of a 16" Meade telescope coupled to various detectors. The beam can be transmitted to the arrays on Tilghman Island and retro-reflected back to the receiver at CBD.

Free-Space Laser Communication and Active Laser Illumination III,
edited by David G. Voelz, Jennifer C. Ricklin, Proc. of SPIE Vol. 5160
(SPIE, Bellingham, WA, 2004) · 0277-786X/04/$15 · doi: 10.1117/12.507701

Report Documentation Page

Form Approved
OMB No. 0704-0188

1. REPORT DATE	2. REPORT TYPE	3. DATES COVERED
2004		**00-00-2004 to 00-00-2004**

4. TITLE AND SUBTITLE	5a. CONTRACT NUMBER
Fast steering mirror implementation for reduction of focal-spot wander in a long-distance free-space communication link	5b. GRANT NUMBER
	5c. PROGRAM ELEMENT NUMBER
6. AUTHOR(S)	5d. PROJECT NUMBER
	5e. TASK NUMBER
	5f. WORK UNIT NUMBER
7. PERFORMING ORGANIZATION NAME(S) AND ADDRESS(ES) **Naval Research Laboratory,Code 8123,4555 Overlook Avenue, SW,Washington,DC,20375**	8. PERFORMING ORGANIZATION REPORT NUMBER
9. SPONSORING/MONITORING AGENCY NAME(S) AND ADDRESS(ES)	10. SPONSOR/MONITOR'S ACRONYM(S)
	11. SPONSOR/MONITOR'S REPORT NUMBER(S)

12. DISTRIBUTION/AVAILABILITY STATEMENT
Approved for public release; distribution unlimited

13. SUPPLEMENTARY NOTES

14. ABSTRACT

15. SUBJECT TERMS

16. SECURITY CLASSIFICATION OF:			17. LIMITATION OF ABSTRACT	18. NUMBER OF PAGES	19a. NAME OF RESPONSIBLE PERSON
a. REPORT **unclassified**	b. ABSTRACT **unclassified**	c. THIS PAGE **unclassified**		**8**	

The receiver consisted of a 16 inch Meade telescope with a focal length of 4 meters. The FSM was mounted at a 45° angle behind the telescope to steer the beam onto the PSD. The PSD was positioned in the focal plane of the Meade with the focal spot approximately in the center of the PSD active area. The beam was transmitted across the bay and the energy retro-reflected back through the telescope to the detector via the FSM. The voltages were then converted to digital signals and stored for later processing. Data was taken with and without the FSM activated.

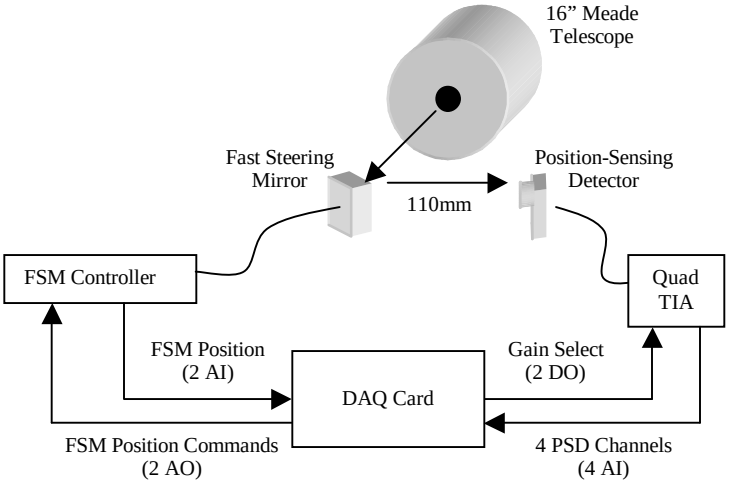

Figure 1: Receiver Block Diagram for characterization of the FSM+PSD beam wander compensation tests. The PSD was positioned in the focal plane of the telescope (f=4 meters) and the received laser light was directed to the PSD via the FSM as shown.

2.1 Fast steering mirror

We used a commercially available fast steering mirror in the experiments. Specifically, we combined with the PSD with the Newport FSM-200. This unit has an optical angular range of ±3° with resolution of ≤ 2μrad rms. Four voice-coil actuators are used to provide a fast, high-bandwidth rotation on two axes of ≥ 550Hz at 100μrad amplitude. The maximum amplitude that the FSM can be driven is limited by the command frequency. The relationship is shown in Figure 2. The FSM controller has four BNC inputs with a ±10V range. Two of the inputs are x and y position commands that were used in the experiment described here. Separate inputs are also available for external feedback of x and y position. The feedback inputs may be used by the controller's internal control loop to drive the feedback input values to zero. However, in this experiment, the command inputs are used to control the FSM and the FSM controller's internal control loop was not used. There are also two BNC outputs with ±10V range. The outputs are the FSM actual x and y positions. The mirror itself has an anti-reflection coating at 1550nm.

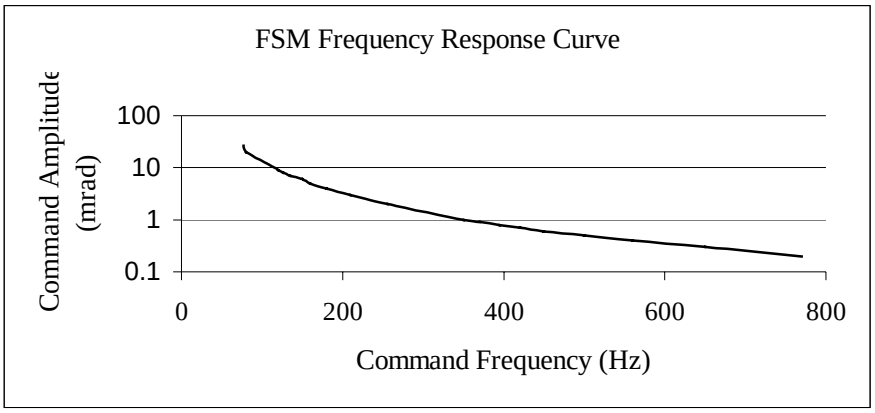

Figure 2: The operating regime for the FSM used in the experiment is shown above.

2.2 Position-Sensing detector

We also used a commercially available PSD for this work. We selected a unit from Judson Technologies. This Germanium device has an active area of 5mm square. Its response at 1550nm is .9-.95 A/W. Table 1 below shows the details of the gain settings for the four PSD channels.

Table 1: Select lines, sensitivity, and bandwidth of the gain settings of the PSD.

A0	A1	Gain (KV/A)	Bandwidth (KHz)
Gnd	Gnd	6.03	79.3
Gnd	+5V	19.135	78.25
+5V	Gnd	60.850	77.45
+5V	+5V	150.384	74.675

On each of the four output channels, x1, x2, y1, and y2, is a matched trans-impedance amplifier.

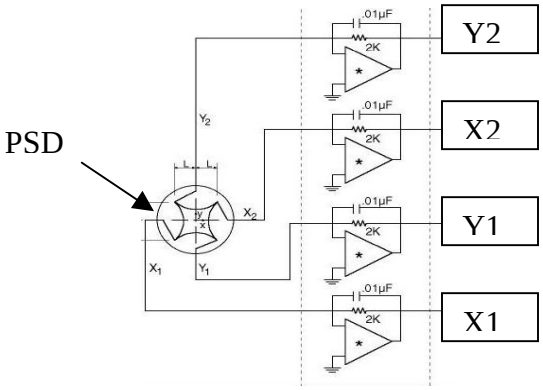

Figure 3: Drawing of the physical positions of the four separate channels on the PSD

Using these four channels, normalized outputs for x and y positions are calculated with the following equations:

$$x/L = (x2 + y2) - (x1 + y1)/(x1 + x2 + y1 + y2) \quad (1)$$

$$y/L = (x2 - y2) - (x1 - y1)/(x1 + x2 + y1 + y2) \quad (2)$$

The curve in Figure 4 converts the values from Eqns (1) and (2) to true focal spot position in millimeters.

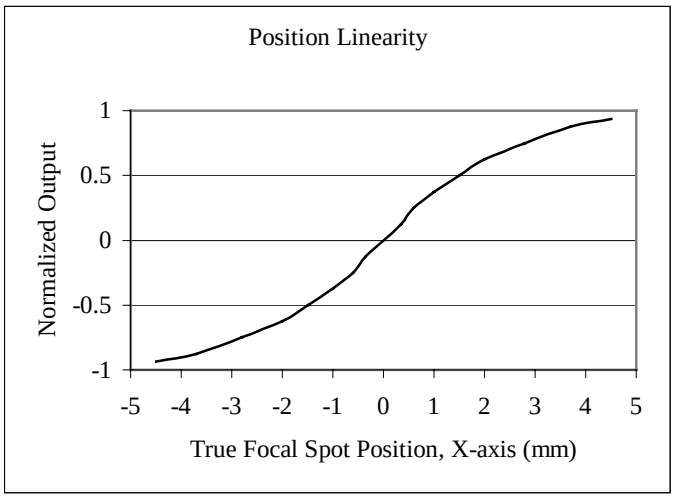

Figure 4: The position linearity curve is shown for the PSD, which is used to convert normalized outputs to true focal spot position.

2.3 Data acquisition and Control

The detected signal was converted to voltages and digitized using a commercially available data acquisition (DAQ) board. The board is capable of analog and digital inputs and outputs, which were used to control the FSM. The PCI DaqBoard/2000 has sixteen 16-bit, 200 KHz analog inputs, two 16-bit, 100KHz analog outputs and 40 digital I/O channels that can be scanned synchronously or asynchronously with analog inputs. The card was also used to read in the voltages of the PSD and control its gain settings.

All of the control loop software was written in the C programming language in the Linux environment on a desktop PC. The algorithm initializes and configures the DAQ card for the analog and digital inputs and outputs. Scan rates are set for the analog inputs, which are read into a circular buffer so that the latest value is always used. Two digital outputs can be used to change the gain setting of the PSD, although the gain did not need to be adjusted for the experiment. The PSD was set to operate at the lowest gain setting. The four channels of the PSD are analog inputs as are the position outputs of the FSM. Because of limitations of the DAQ card, the inputs could only be read from the buffer at 100Hz. This was the limiting factor in the control loop bandwidth. The scan rate however, could be much higher. To reduce noise, fifteen values were read each time the buffer was accessed and the average of those fifteen values was used to determine the position from the PSD. The PSD values, converted to millimeters, indicated the error to be corrected by the FSM. The PSD was located about 110mm from the FSM and the FSM moved 2.6mrad/V, so the following equations determined the voltage to be applied to the FSM:

$$\theta = \tan^{-1}(\mathrm{PSDx}/110) \qquad (3)$$

$$\mathrm{Volts} = \theta / .0026 \qquad (4)$$

PSDx is the actual x position on the PSD in millimeters. θ is the angle in radians that the FSM needs to move. Sign conventions were experimentally defined and were sent to the FSM to drive the PSD positions to zero. In addition, there were errors due to slight misalignments of the axes of the FSM and the PSD. An estimate of the static transfer function needed for correct positioning of the beam was determined experimentally. The actual voltage sent to command the FSM was an average of the last two PSD positions

to ensure that the FSM was not being overdriven. This was necessary, since the amplitude of the FSM motion decreases as command frequency increases. All required calculations and computer interface I/O were completed in approximately a millisecond. Therefore, the 100 Hz access frequency of the analog input buffer on the DAC card was the limiting component in control loop speed.

3. DATA AND RESULTS

The main goal of this effort is to correct for beam wander at the detector, which causes power loss in a free-space optical communication link. Figure 4 shows an example of the motion of the received energy at the focal plane of the telescope detected by the PSD. The data was collected at a 4 kHz acquisition rate over a period of 125 seconds[1]. The angle-of-arrival variance was 519 μrad[2]. These values are typical for daylight hours in the Chesapeake Bay region.

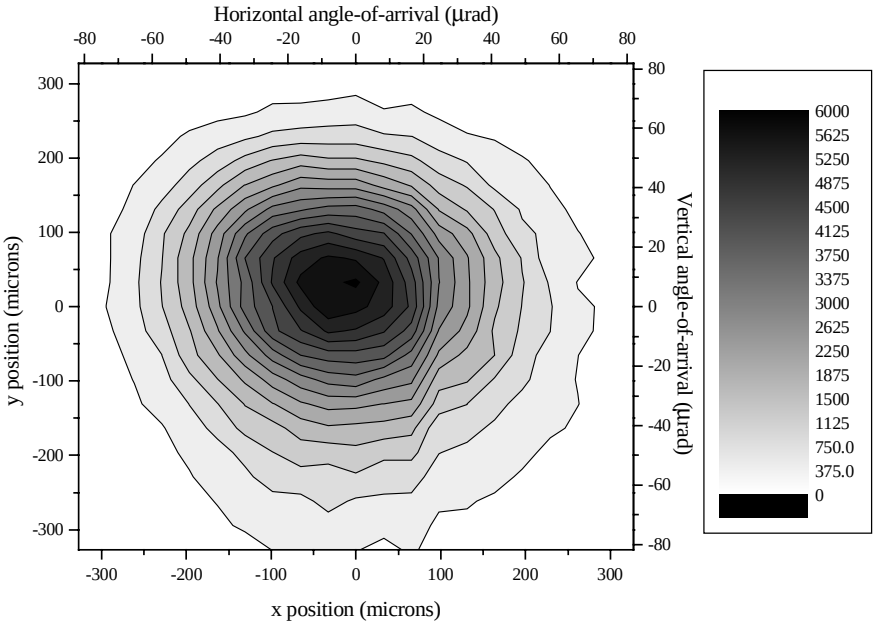

Figure 4: Histogram of the received spot centroid over 2 minutes of acquisition time. The intensity/contours scale is the number of counts received within each bin of the histogram. 21 bins were used in each axis to generate the histogram. The x and y position scales are physical position on the surface of the PSD. The vertical and horizontal angle-of-arrival scales are the angle-of-arrival into the telescope, which are calculated based on the 4-meter focal length of the telescope.

To compare the performance of the system to an uncorrected baseline, data was taken during the early morning when atmospheric turbulence was very low. The propagation path was horizontal so the expected stronger influence in the vertical direction from turbulence was mitigated by time-of-day. Figures 5 and 6 compare data without and with FSM control. In Figure 5, the spot centroid fluctuates 100-125 microns over a 3-minute period. This variation is much smaller than what is expected during daylight hours with moderate turbulence as shown above in Figure 4. In Figure 6, we can see improvement with active FSM correction. . The centroid now fluctuates by only ~75 microns. The spot is also centered much closer around (0,0) on the PSD.

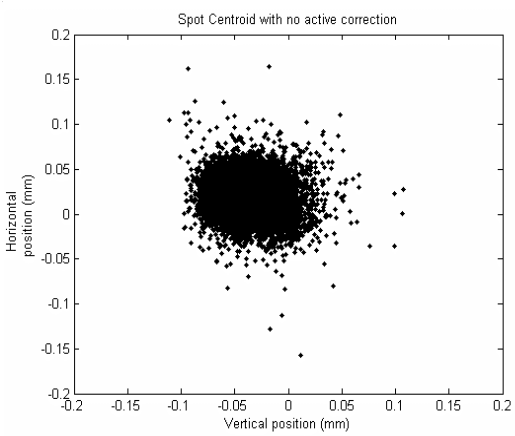

Figure 5: Spot centroid motion over 3 minutes with no correction by the FSM. The horizontal and vertical scales correspond to real space.

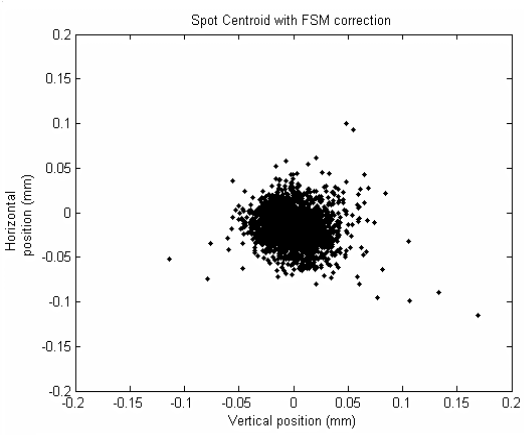

Figure 6: Spot centroid motion over 3 minutes with active correction by the FSM. The horizontal and vertical scales correspond to real space.

Histograms were generated from the data to compare the distance of the spot centroid from the mean with and without FSM correction. These plots are shown in Figures 7 and 8. Figure 7 has no FSM correction and has an average distance from the mean of 40 microns. Active FSM correction yields an average distance from the mean of just 20 microns, shown in Figure 8.

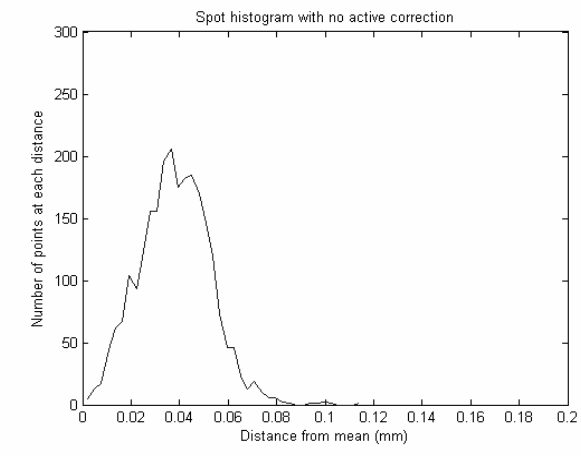

Figure 7: Histogram of the received spot centroid over a 3-minute period with no active FSM correction. Distance from the mean was calculated for all points to generate the histogram.

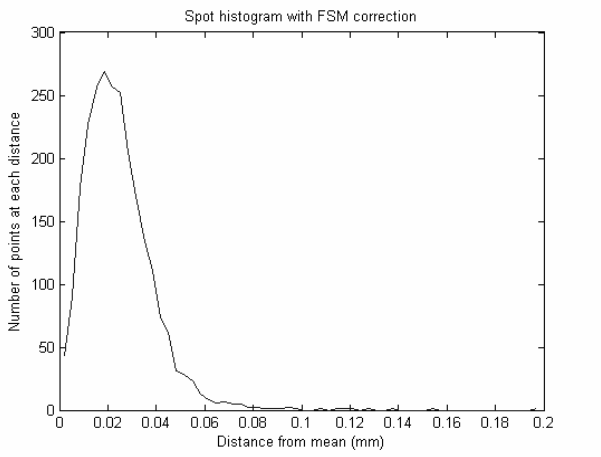

Figure 8: Histogram of the received spot centroid over a 3-minute period with active FSM correction. Distance from the mean (x, y) was calculated for all points to generate the histogram.

Quality of the data for the initial set of parameters can be judged from the compared power spectral densities. These are shown in Figure 9. These graphs are calculated from the y position data from the PSD with and without active FSM correction. As can be seen from the plots, the comparison shows a slight improvement; however, this was the first attempt at using the FSM and the control loop parameters are not yet optimized.

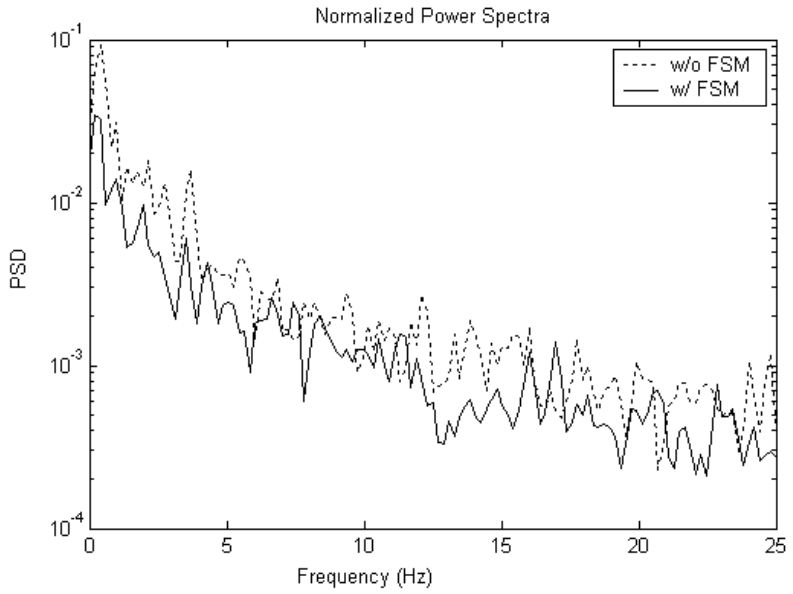

Figure 9: Comparison of the normalized power spectra for y position data with and without FSM correction.

4. CONCLUSIONS AND FUTURE WORK

Implementing a fast steering mirror to actively compensate for angle-of-arrival fluctuations will improve focal spot position stability hence receiver performance for an optical data link. These experimental results loop exhibit such improvement in spot position stability. These are preliminary results as there are a number of parameters needed to optimize the performance. In addition to parameter optimization, we intend to install a new analog input card to increase the loop bandwidth to at least 1 kHz. This upgrade promises to enable compensation for the majority of the atmospheric turbulence.

Another approach that will be pursued is to use the FSM internal control loop. This implementation will require that the PSD output signals be conditioned properly so they can serve as feedback to the FSM controller. Future plans also include integration of a beam splitter into the optical path to direct the most of the received light into either multimode or single mode fiber and lens Bit error rate performance will be examined with and without closed loop control of the FSM.

REFERENCES

1. C.I. Moore, H.R. Burris, M.R. Suite, M.F. Stell, M.J. Vilcheck, M.A. Davis, W.R. Smith, R. Mahon, W.S. Rabinovich, J.P. Koplow, W.J.Scharpf, and A.E. Reed, "Free-space high-speed laser communication link across the Chesapeake Bay", *SPIE Proc.*, 4821, pp. 474-485, 2002.

2. M.J. Vilcheck, H.R. Burris, C.I. Moore, M.F. Stell, M.R. Suite, M.A. Davis, R. Mahon, E. Oh, W.J. Scharpf, W.S. Rabinovich, A.E. Reed, and G.C. Gilbreath, "Progress in high-speed communication at the NRL Chesapeake Bay lasercomm facility", *SPIE Proc.*, 2003, This issue.

3. F. Di Teodoro, J.P. Koplow, S.W. Moore, "Diffraction-limited, 300-kW peak-power pulses from a coiled multimode fiber amplifier", *Optics Letters* **27(7)**, pp. 518-20, 2002.

4. J.P. Koplow, S.W. Moore, D.A.V. Kliner, "A new method for side pumping of double-clad fiber sources", *IEEE Journal of Quantum Electronics*, **39(4)**, pp. 529-40, April, 2003.